Iraqi J. Laser, issue 2, vol., 20, pp. 24-31 (2021)

IRAQI JOURNAL OF LASER

# Experimental Study to The Effect of Applying Stressing Force on Etched Polarization Maintaining Fiber as Hybrid Fabry-Perot /Mach-Zehnder inline fiber interferometer

**Nada F. Noori [1], Tahreer S. Mansoor [1]**

**Corresponding author: Tahreer@ilps.uobaghdad.edu.iq*

1. *Institute of Laser for Postgraduate Studies, University of Baghdad, Iraq, Baghdad, Iraq.*

(Received 27/10/2021; accepted 29/12/2021)

**Abstract:** The increased interest in developing new photonic devices that can support high data rates, high sensitivity and fast processing capabilities for all optical communications, motivates a pre stage pulse compressor research. The pre-stage research was based on cascading single mode fiber and polarization maintaining fiber to get pulse compression with compression factor of 1.105. The demand for obtaining more précised photonic devices; this work experimentally studied the behavior of Polarization maintaining fiber PMF that is sandwiched between two cascaded singe mode fiber SMF and fiber Bragg gratings FBG. Therefore; the introduced interferometer performed hybrid interference of both Mach-Zehnder and Fabry-Perot interferometers. The hybrid interference is resulted from the interference of the forward, backward and X,Y polarization components of the propagating light along the cascaded fibers. In conclusion spectral pulse compression with maximum compression factor in range of 3-6 was obtained by tuning applied stress on the shortest etched PMF segment of the interferometer (i.e. 8cm length). Such interferometer can support fine tunable all optical band pass filter

**Key words:** inline fiber interferometer, polarization maintaining fiber, HF fiber etching, Mach-Zehnder interferometer

## 1. Introduction

Hybrid Inline fiber interferometers are trending among the recent research areas due to their attractive advantages of light weight, compact size, immunity to electromagnetic interference [1], signal modulation capability, pulse compression [2], simultaneous sensing capability of two or more measured and, compatibility with fiber-based systems [3]. Moreover; current trends in fiber optic interferometers is to minimize the device for micro-scale applications. Since the interferometers provide a lot of temporal and spectral information, the detected signal can be quantitatively determined by various means for detecting the changes in the wavelength, phase, intensity, frequency, bandwidth, and so on [4]. With these sensing indicators, they achieved remarkable performance with large dynamic range, high accuracy, and high sensitivity [5]. Hybrid inline fiber interferometer usually can be built by cascading more than one type of interpolated misalignment along the optical bath of the fiber. such misalignment was ensured in previous studies by both cascading different types of optical fibers and imposing a reflective cross-sectional surface in addition to tapering of two or more regions along the same optical fiber...etc. and in our previous work [6-9]. Polarization maintaining fibers PMF are generally used to eliminate the effect of polarization mode dispersion along optical fibers. Polarization mode dispersion usually alter the phase of the propagating mode along the optical fiber [9]. Hybrid inline fiber interferometer were implemented in pre-stage work by sandwiching multi-mode fiber between two single mode-fiber Bragg gratings [8]a very fine tuned optical filter was obtained while PMF sandwiched between two single mode fibers was used to build Mach-Zehnder interferometer PM-

MZI [10]. The introduced PM-MZI worked as goon pulse compressor with pulse compression factor of 1.103 compression [2],[10]. While compression factor of 0.99 were ensured after our pre-stage work using photonic crystal fiber [11].

Fabry-Perot interferometer (FPI) sensors are widely used in a variety of fields that range from industry to biochemistry has become an attractive choice for force and strain sensing for their compact structure, high sensitivity, flexibility and small cross sensitivity. Through the strain experiment, they found that the interferometer with a larger cavity has a higher strain sensitivity.[12],[13],[14]

This work experimentally studied the effect of applying mechanical stressing force on etched polarization maintaining fiber sandwiched between two FBG cavity to produce hybrid Fabry-Perot Mach-Zehnder inline fiber interferometer. Since the two identical highly reflecting FBG (>90%) operates as Fabry-Perot cavity and the cascaded structure that consists from etched polarization maintaining fiber between two single mode fiber works as Mach Zehnder interferometer. Five different mass weights were used to apply mechanical stress along the etched PMF and thus the resulted change in optical power, central wavelength shift and spectral width were recorded.

## 2. Method and procedure

Hybrid inline fiber interferometer occurs when interference pattern obtained along the optical fiber due to more than one mechanism[15][16]. In this work hybrid inline fiber interferometer is obtained from two types of interferometers in one structure. The first type is the Mach-Zehnder interferometer which is implemented using 20 min etched polarization maintaining fiber of three different lengths (8,16, and 24 cm) sandwiched between two single mode fibers of 10 cm length. Since the polarization maintaining fiber has a beat length $L_B$ characteristic which defines the length that polarization components of the propagating light will be remained separated along the fiber[9],[17]. The $L_B$ of the used PMF (Thorlabs- PMDCF) in this work is equal to 5mm and hence interference between the different polarization components will be occurred after 5mm along the second single mode fiber. In addition to polarization components interference we have the evanescent wave obtained on the edges of the etched region of the PMF which develops some unguided waves propagating in the clad of the PMF at the etched zone resulting from the difference of the effective refractive index of the fiber at that zone, these unguided more recombined as guided modes again when they enter the second not etched segment of the PMF[18],[19]. The second interferometer type in this work is the Fabry-Perot inline fiber interferometer resulted from the interference of the forward and backward light waves reflected between the two identical fiber Bragg gratings applied on the both sides of the previously mentioned Mach-Zehnder interferometer as shown in the experimental schematic diagram of figure (2). The interference pattern of any interferometers can simply be described by the general interference formula expressed in equation Error! Reference source not found.. The developed phase change along each separated Mach-Zehnder arm of this work can be expressed by equation Error! Reference source not found. [6],[21]-[22]

$$\mathbf{H(\lambda) = I_1(\lambda) + I_2(\lambda) + 2\sqrt{I_1(\lambda)I_2(\lambda)}\cos(\Delta\varphi)} \dots\dots\dots\dots\dots\dots\dots\dots\dots\dots (\mathbf{1})[23]$$

$$\boldsymbol{\varphi = \frac{\omega \Delta n_{eff} L}{c}} \dots\dots\dots\dots\dots\dots\dots\dots\dots\dots (\mathbf{2})[23]$$

Where $I_{1,2}$ represent the intensity of interfering light beams as a function of wavelength and φ represent the phase change of the interfering waves and it is a function of effective refractive index change $\Delta n_{eff}$, angular frequencyω, wavelength λ and optical path length L.

Beat length $L_B$ of the polarization maintain fiber is directly related to the birefringence B can be calculated using equation Error! Reference source not found.. The birefringence B of the used PMF in this work is equal to 2.5 x $10^{-4}$

$$\boldsymbol{LB = \frac{2\pi}{\Delta\beta} = \frac{\lambda}{B}} \dots\dots\dots\dots\dots\dots\dots\dots\dots\dots (\mathbf{3})[\mathbf{9}]$$

$$\boldsymbol{B = \Delta n_{eff} = n_{eff}^{x} - n_{eff}^{y}}[9]$$

Where Δβ is the difference between the two x and y components of wave propagation constant along the PMF and $n^{x,y}_{eff}$ is the effective refractive index as a function of wavelength for both x and y polarization component. The inline Mach-Zehnder interferometer at this work was designed according to phase equation (2); thus the Beat length 5mm gives phase difference N×75°, and three PMF lengths of 8cm, 16 and 24 which gives phase difference of N×58 ° and N×63°.

For hybrid interference the interference of each type of interferometer needs to be represented mathematically in separated formula thus the Mach-Zehnder interference is represented by equation (5) and the Fabry-Perot one is represented by equation (6) [24]

$$I_{MZ} = I_1 + I_2 + 2\sqrt{I_1 I_2}\cos\left(\frac{2\pi n_{eff} L_{mzi}}{\lambda}\right) \dots\dots\dots (5)$$

$$I_{FP} = I_{FW} + I_{BW} + 2\sqrt{I_{FW} I_{BW}}\cos\left(\frac{4\pi n_{eff} L_{FPI}}{\lambda}\right) \dots (6)$$

where, $I_1$ and $I_2$ are the intensity of the core and cladding mode, respectively. $I_{FW}$ and $I_{BW}$ are the forward and backward reflected light intensities between FBGs respectively. $\Delta n_{eff} = n_{eff}^{core} - n_{eff}^{clad}$ effective refractive index difference between core mode and cladding mode. $L_{mzi}$ and $L_{FPI}$ are the length of Mach-Zehnder interferometer and Fabry-Perot cavity respective which are equal to 28,36 and 44 for the MZI and 78,86,94 cm for the FPI.

The applied force on the PMF was done using series of different weight masses laid side by side along the etched zone of the PMF. Since the etched region is very brittle therefore to protect it from being raptured or damaged a thin slice of glass was used to isolate the weight mass and uniformly distribute their stressing effect on the PMF. The applied weights with their equivalent force in Newton are shown in table (1)

***Error! Reference source not found.***): The Equivalent force of the applied weight masses on the PMF cross-sectional

| Weight in (g) | Force (N) |
|---|---|
| 0 | 0 |
| 40 | 0.392266 |
| 80 | 0.784532 |
| 150 | 1.470997 |
| 300 | 2.941 |

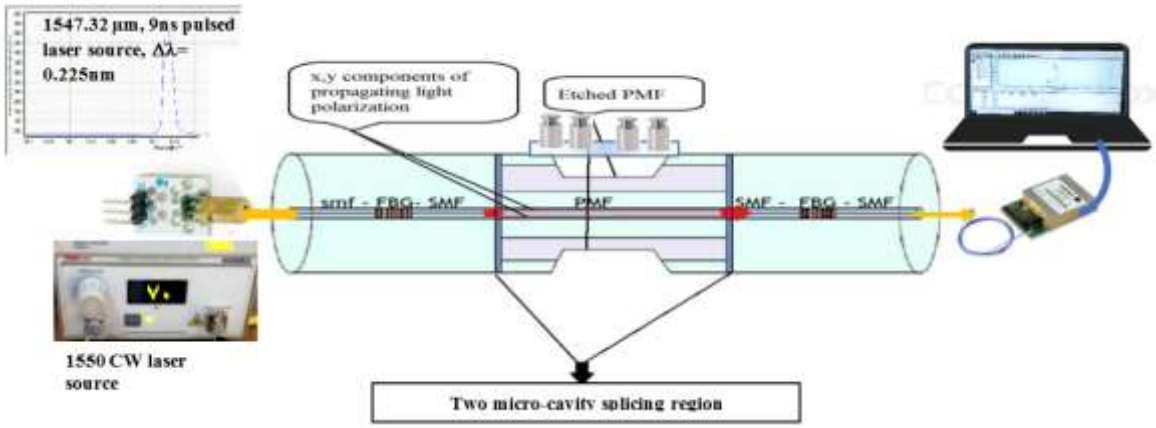


**Figure (1):** The schematic diagram of the experimental set up

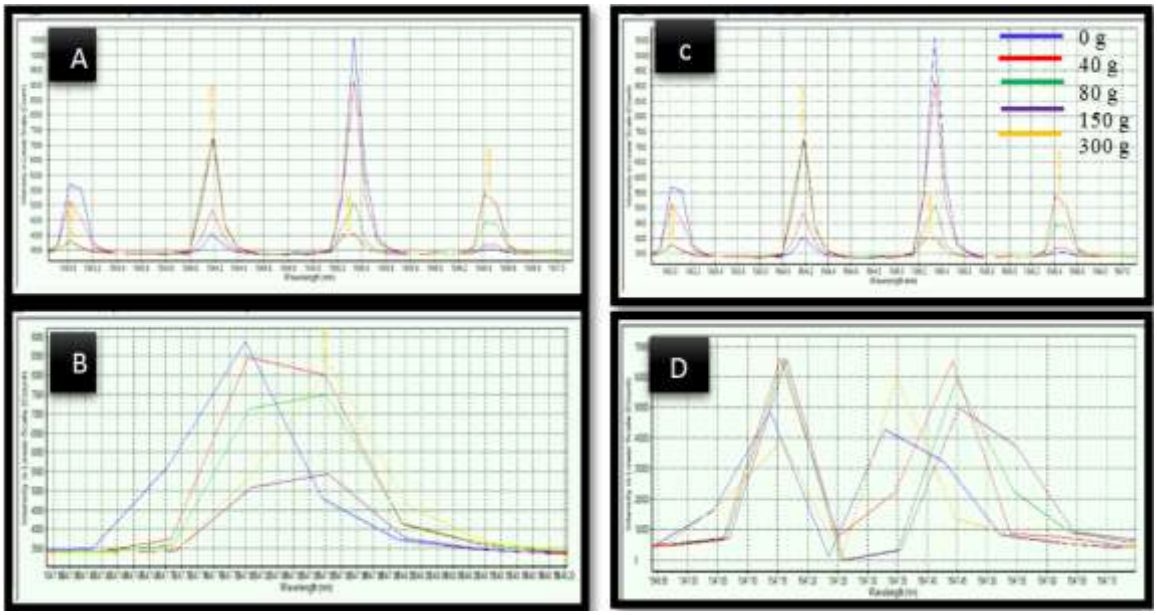

**Figure (2):** The spectrum of the experimental measurement output signal from the interferometer using FBGA interrogator. A: for the CW laser source and 8cm PMF, B: for pulsed laser diode and 8cm PMF, C: CW Laser with 16 cm PMF, D: pulsed laser and 16 cm PMF

The Experimental procedures were carried for two different types of C-band laser sources the first one is pulsed laser diode has central wavelength of 1547.32µm, 9ns pulse duration, 0.225nm spectral width and 1.33 mW peak power as shown in figure (2-a). while the CW laser has five peaks centered at 1542-1550 nm with 2nm spacing between each two consequent peak. The peak power obtained from the CW laser can be tuned from 0.2 to 0.9 mW but power of 0.7 mW was applied to the structure. The Fabry-Perot cavity was implemented using two identical fiber Bragg gratings of 1546.7 nm central wavelength, 90% reflectivity, 10 mm the grating segment length is 0.2 nm bandwidth The used spectral visualizer was FBGA interrogator (Bayspec) as shown in figure (2). In order to homogenously apply mass of 40 g along the etched region of the PMF; 4 masses of 10 g reference value was lied side by side next to each other along almost 4 cm of the etched fiber. the preparation of etched segment was explained in our previous work [7] by using HF bath of 4 cm length and hence there is an error percent raised from not all the clad was removed with same amount because the manual control to etching period is considered as source of error besides the cleaning of the sample after etching can take slightly different duration in seconds range they can be the second source of error

## 3. Results and discussion

The resulted effect of the stressing elements on the hybrid interferometer was investigated in term of central wavelength, spectral width, and Peak power variation as shown in figures (3-5) By looking for the central wavelength shift under the effect of stressing weight; it is obvious that there is almost no magnificent shift. Most cases are of nearly same central wave length except the case of FBG- cavity with CW laser source the fluctuation toward the shorter wavelengths were occurring as a result of the increasing of the applied stress.

The proposed advantage of using the FBGs around the both ends of the PMF is to produce the hybrid interference between forward and backward wave with PM-MZI interferometer. Thus Fabry-Perot cavity operation can be obtained. Then expected behavior of such hybrid interferometer is to increase the quality of the signal obtained from stress detection region along the etched PMF and obtain higher power from the interferometer. But unfortunately according to figures (3-5) (a) we can see that FBG cavity decreased the power of the hybrid interferometer FP-PMMZI incredibly. However still the Fabry Perot cavity showed feasible change to the pulse width (FWHM) against the applies stress when it is compared with the case of PM-MZI alone without cavity.

The central wavelength change was very slight in the most cases except for the 24 cm PM-MZI and 24 cm FP-PMMZI we can see slight obvious red-shift.

Spectral pulse compression of were obtained with highest compression factor ($FWHM_{i/p}$/ $FWHM_{o/p}$) of 6.818 with the shortest cavity of 8cm PMF length but range between 1-3 spectral compression were obtained from the whole structure as shown in Table (2- a & b)

**Table (2)**: The spectral pulse compression factor with respect to applied stress in case of (a) No Fabry Perot Cavity, (b) Fabry Perot Cavity

| | *(a)* No Fabry –Perot Cavity | | | (b) Fabry –Perot Cavity | | |
|---|---|---|---|---|---|---|
| **Force (N)** | ***8cm PMF*** | ***16 cm PMF*** | ***24cm PMF*** | ***8cm PMF*** | ***16 cm PMF*** | ***24cm PMF*** |
| ***0*** | 1.44230769 | 0.81227437 | 1.53061224 | 1.65441176 | 0.80357143 | 1.70454545 |
| ***0.392266*** | 1.28571429 | 0.86538462 | 3.125 | 2.08333333 | 0.76013514 | 1.99115044 |
| ***0.784532*** | 3 | 0.74013158 | 1.63043478 | 4.32692308 | 0.76271186 | 0.80357143 |
| ***1.470997*** | 4.24528302 | 0.9 | 2.16346154 | 4.32692308 | 1.99115044 | 3.16901408 |
| ***2.941*** | 3.62903226 | 0.74013158 | 1.74418605 | 6.81818182 | 2.10280374 | 1.875 |

The tunable spectral width of the interferometer can be used as tunable band pass filter that can be tuned over very fine range in nm regime for the used laser in this study tuning range of the spectral pulse was between 0.1-0.3 nm.

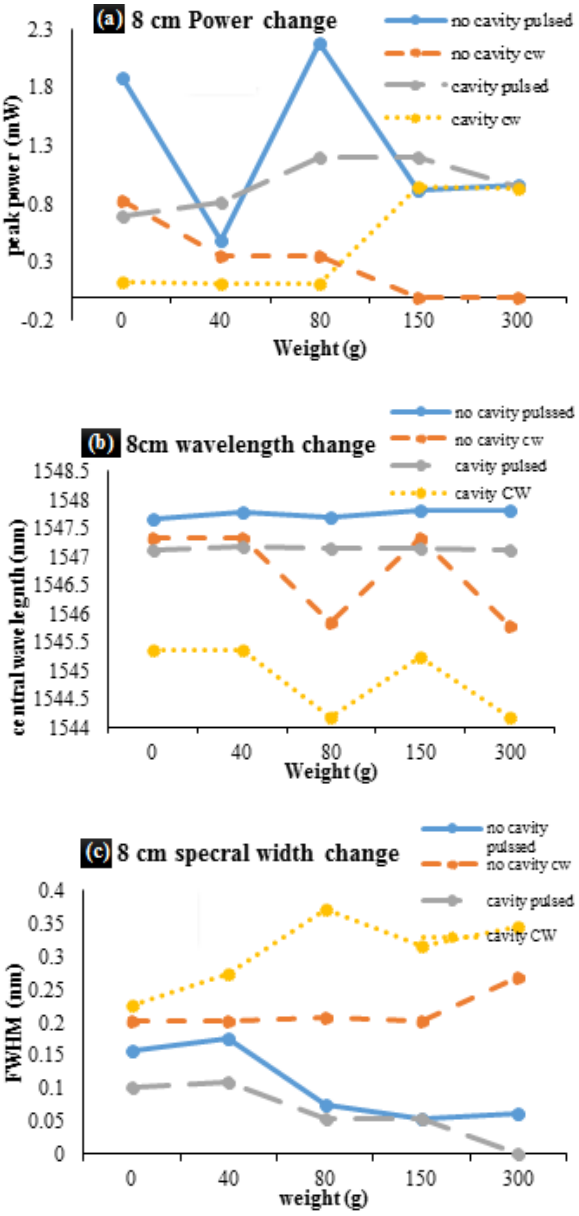


**Figure (3):** The effect of stressing weights on the 8cm PM-MZI. (a) power change, (b) wavelength change and (c) is the FWHM change with respect to stress

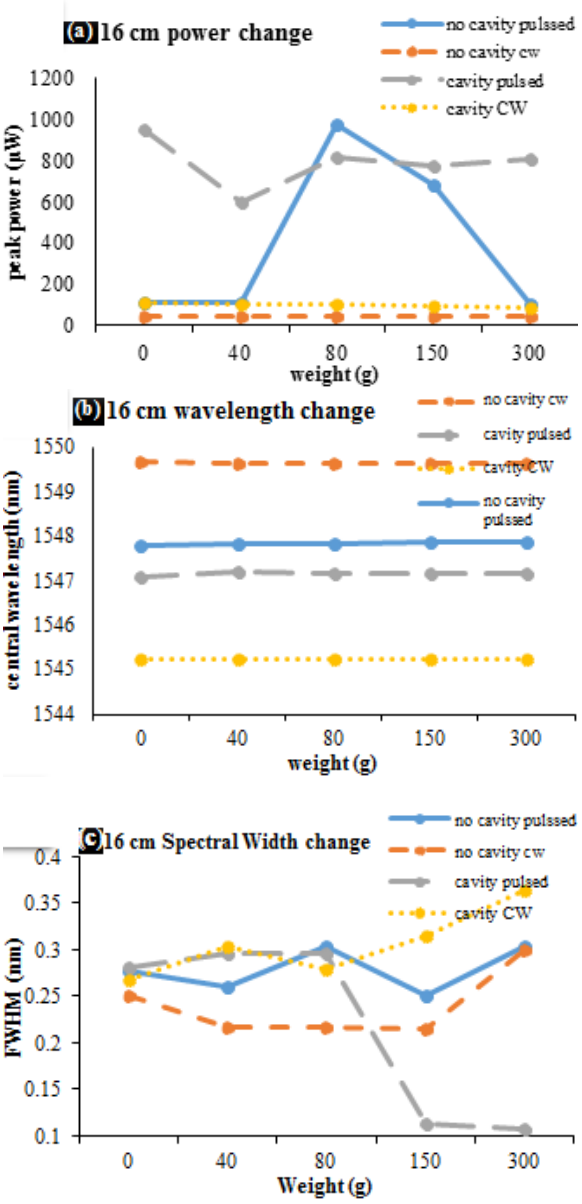


**Figure (4):** The effect of stressing weights on the 16 cm PM-MZI. (a) power change, (b) wavelength change and (c) is the FWHM change with respect to stress.

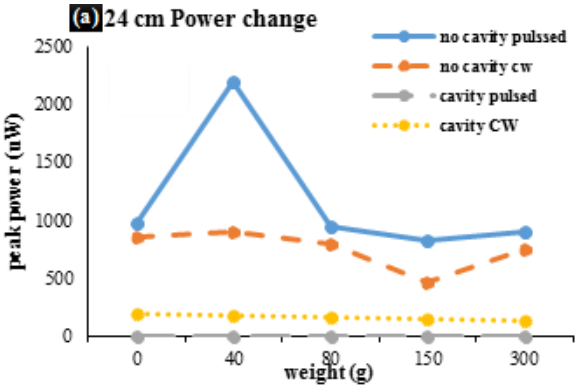

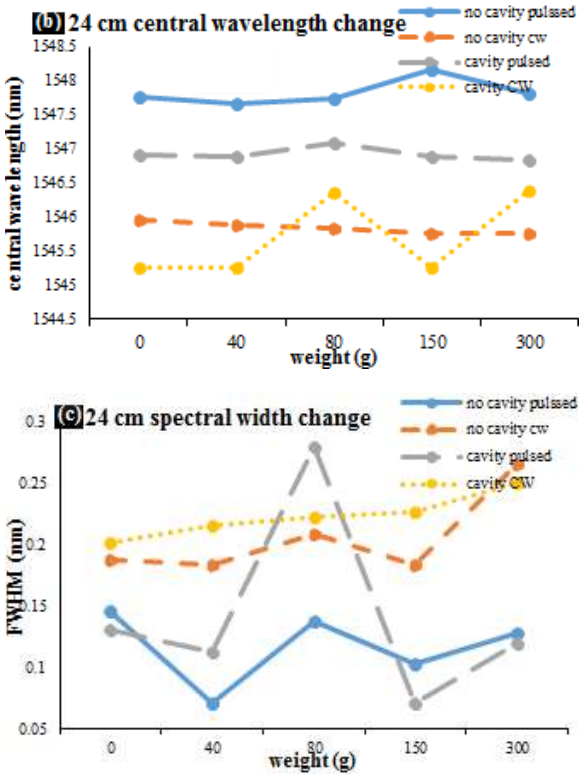


**Figure (5):** The effect of stressing weights on the 24 cm PM-MZI. (a) power change, (b) wavelength change and (c) is the FWHM change with respect to stress

## 4. Conclusions

This paper studied experimentally the effect of stressing Hybrid Fabry-Perot/ Mach-Zehnder interferometer consists from polarization maintaining fiber, single mode fiber and fiber Bragg grating and in conclusion it was found that Fabry-Perot cavity reduced the wavelength shift that should have occurred under stress and out power is reduced significantly. In contrast to previous PM-MZAI [2]; this FP-PMMZI developed temporal dispersion to optical pulse and significant spectral pulse width compression with tunable compression factor that increases by increasing the applied tuning stress. Therefore tunable all optical spectral band pass filter was obtained.

## 5. References

[1] Zhu, T., Wu, D., Liu, M., & Duan, D. W. In-line fiber optic interferometric sensors in single-mode fibers. Sensors, **12**, (8), pages 10430 – 10449. Switzerland (2012). https://doi.org/10.3390/s120810430

[2] Mutar, B. H., Noori, N. F., Hammadi, Y. I., & Mansour, T. S. In-line fiber tunable pulse compressor using PM-Mach Zehnder interferometer, Journal of Mechanical Engineering Research and Developments, **44,** (5), 287–297 (2021).

[3] Li, L., Xia, L., Xie, Z., Hao, L., Shuai, B., & Liu, D. In-line fiber Mach-Zehnder interferometer for simultaneous measurement of refractive index and temperature based on thinned fiber. Sensors and Actuators, A: Physical, **180,** 19–24. (2012).https://doi.org/10.1016/j.sna.2012.04.014

[4] Korposh, S., James, S. W., Lee, S. W., & Tatam, R. P.. Tapered Optical Fibre Sensors: Current Trends and Future Perspectives. Sensors (Switzerland), **19**(10). (2019) https://doi.org/10.3390/s19102294

[5] Bal, H. K., Brodzeli, Z., Dragomir, N. M., Collins, S. F., & Sidiroglou, F. Uniformly thinned optical fibers produced via HF etching with spectral and microscopic verification. Applied Optics, **51**(13), 2282–2287. (2012). https://doi.org/10.1364/AO.51.002282

[6] Krzysztof Iniewski, "OPTICAL FIBER SENSORS, Advanced Techniques and Applications", Taylor & Francis Group, 2015 International Standard Book Number-13: 978-1-4822-2829-8 (eBook - PDF)

[7] Tahreer S. Mansoor, N. F. N. (2021) "Theoretical and Experimental Study to The Effect of Etching on Polarization Maintaining Fiber of Mach-Zehnder interferometer", Design Engineering, pp. 6973-6981. Available at: http://www.thedesignengineering.com/index.php/DE/article/view/4188 (Accessed: 16October2021).

[8] Tahreer S. Mansour, N. F. N. (2021). Design and Construction of Tunable Band Pass Filter Using Hybrid FPMZI. Design Engineering, 6959-6972. Retrieved from http://www.thedesignengineering.com/index.php/DE/article/view/4187

[9] Ivan P. Heckman, Alan E. Willner, "optical fiber telecommunications" Academic Press is an imprint of Elsevier, California 92101-4495, USA Theobald's Road, London WC1X 8RR, UK, ISBN: 978-0-12-374171-4

[10] Mutar, B. H., & Mansour, T. S. "Design of Tunable Optical Band Pass Filter based on in-Line PM- Mach Zehnder Interferometer". Iraqi Journal of Laser, **20**(1), pp. 6-12. (2021). Available at:

https://ijl.uobaghdad.edu.iq/index.php/IJL/article/view/257 (Accessed: 22August2021).
[11] Wang, X., Liao, J., Pan, J., Yang, H., & Li, X. (2021). Observation of Ultrashort Laser Pulse Evolution in a Silicon Photonic Crystal Waveguide. 2–7.
[12] Guozhao Wei, Qi Jiang, Force sensitivity and fringe contrast characteristics of spheroidal Fabry-Perot interferometers. Optics express vol. 28, issue 17, page 24586–24598. 2020
[13] Chyad, R. M., Ali, A. H., Hammed, A. A., Mahdi, B. R., Khalef, N. H., Mahmoud, A. I., & Rasheed, H. M.. Acoustic Fiber Sensors by Fabry- Perot Interferometer technology. Journal of Physics: Conference Series, 1660(1). (2020) https://doi.org/10.1088/1742-6596/1660/1/012052
[14] Xu, Y., Lu, P., Chen, L., & Bao, X. Recent developments in micro-structured fiber optic sensors. Fibers, 5(1). (2017). https://doi.org/10.3390/fib5010003.
[15] Peng, W., Zhang, X., Gong, Z., & Liu, Y.. "Miniature fiber-optic strain sensor based on a hybrid interferometric structure". IEEE Photonics Technology Letters, 25(24), 2385–2388. (2013) https://doi.org/10.1109/LPT.2013.2284965
[16] Wang, J., Liu, B., Wu, Y., Mao, Y., Zhao, L., Sun, T., Nan, T., & Han, Y. Temperature insensitive fiber Fabry-Perot / Mach-Zehnder hybrid interferometer based on photonic crystal fiber for transverse load and refractive index measurement. Optical Fiber Technology**,** **56** 7–13. (November 2019), https://doi.org/10.1016/j.yofte.2020.102163
[17] John Senior, M. Yousif Jamro," Optical Fiber Communications Principles and Practice", Third edition, Prentice Hall Europe, 2009, ISBN: 978-0-13-032681-2
[18] Patil, S. H., Saha, A., & Barma, M. D. Performance analysis of cladding etched fiber Bragg grating based refractive index sensor. 2018 2nd International Conference on Electronics, Materials Engineering and Nano-Technology, IEMENTech 2018, 6, 1–3. https://doi.org/10.1109/IEMENTECH.2018.8465251
[19] Kumar, A., Single Mode Optical Fiber based Refractive Index Sensor using Etched Cladding. 0–4. 2011https://doi.org/10.21427/wh9t-ce84
[20] Flores, R., Janeiro, R., & Viegas, J. Optical fiber Fabry-Pérot interferometer based on inline micro cavities for salinity and temperature sensing. Scientific Reports, 9(1), 1–9. (2019) https://doi.org/10.1038/s41598-019-45909-2
[21] Series Editors Paul L. Kelley, Ivan P. Kaminow, Govind P. Agrawal, "Applications of Nonlinear Fiber Optics", Academic press, ISBN:0-12-045144-1, https://doi.org/10.1016/B978-0-12-374302-2.X5001-3
[22] Li, L., Xia, L., Xie, Z., Hao, L., Shuai, B., & Liu, D. In-line fiber Mach-Zehnder interferometer for simultaneous measurement of refractive index and temperature based on thinned fiber. Sensors and Actuators, A: Physical, 180, 19–24. (2012). https://doi.org/10.1016/j.sna.2012.04.014
[23] Zhu, C. C., Yu, Y. Sen, Zhang, X. Y., Chen, C., Liang, J. F., Liu, Z. J., Meng, A. H., Jing, S. M., & Sun, H. B. Compact Mach-Zehnder interferometer based on tapered hollow optical fiber. IEEE Photonics Technology Letters, 27(12), 1277–1280. (2015). https://doi.org/10.1109/LPT.2015.2417212
[24] Wang, J., Liu, B., Wu, Y., Mao, Y., Zhao, L., Sun, T., Nan, T., & Han, Y. Temperature insensitive fiber Fabry-Perot /Mach-Zehnder hybrid interferometer based on photonic crystal fiber for transverse load and refractive index measurement. Optical Fiber Technology, 56, 7–13. (2020). https://doi.org/10.1016/j.yofte.2020.102163

# دراسة عملية لتأثير الاجهاد المسلط على ليف بصري مستقطب محفور مستخدم لبناء مداخل ضوئي خطي ليفي هجين بين نوعي ماخ زندر وفابري بيروت

ندى فارس نوري  د. تحرير صفاء منصور

معهد الليزر للدراسات العليا – جامعة بغداد

**الخلاصة:** الحاجة المتزايدة لتطوير أجهزة فوتونية لها القدرة على نقل إشارات الاتصالات الضوئية بكميات كبيرة وسرع عالية حفز لتقديم هذا البحث الذي يعتبر تتمة الى بحث سابق مبني بنفس الالياف وتمكن من تحقيق ضغط للبضة البصرية بمعامل ضغط مقداره 1.105. هذا البحث قدم دراسة عملية لمداخل ضوئي خطي مبني على تعاقب الالياف الضوئية وقد استخدم لغرض الدراسة ليف بصري احادي النمط على جانبي ليف بصري مستقطِب للضوء وحصر الجميع بليف بصري محزز نوع براغ ليقوم بعمل هجين بين نوعين من المدخلات الضوئية نوع فابري بيروت وماخ زندر معا. يتحقق المداخل نوع ماخ زندر من تداخل موجتين ذات استقطاب مختلف اما النوع الثاني من المداخلات وهو فابري بيروت فيتحقق نتيجة لتداخل الموجة الساقطة والمنعكسة على حزوز الليف المحزز. تمكن هذا النوع الهجين من المداخلات الليفية الخطية من تحقيق انضغاط طيفي للموجة الخارجة منه بمعامل انضغاط يتراوح بين 3-6 وسجل اعلى انضغاط مع أقصر طول لليف المستقطب للضوء وهو 8سم كما وتم تمكين تعيير الانضغاط للموجة بتسليط اجهاد على المنطقة المحفورة من الليف.